



RIDDLED BASINS AND UNSTABLE DIMENSION VARIABILITY IN CHAOTIC SYSTEMS WITH AND WITHOUT SYMMETRY

RICARDO L. VIANA

*Departamento de Física, Universidade Federal do Paraná,
Caixa Postal 19081, 81531-990, Curitiba, PR, Brazil*

CELSO GREBOGI

*Instituto de Física, Universidade de São Paulo,
Caixa Postal 66318, 05315-970, São Paulo, SP, Brazil*

Received October 2, 2000; Revised November 21, 2000

Riddling occurs in dissipative dynamical systems with more than one attractor, when the basin of one attractor is punctured with holes belonging to the basins of the other attractors. The basin of a chaotic attractor is riddled if (i) it has a positive Lebesgue measure; (ii) in the vicinity of every point belonging to the basin of the attractor, there is a positive Lebesgue measure set of points that asymptote to another attractor. We investigate the presence of riddled basins in a two-dimensional noninvertible map with a symmetry-breaking term. In the symmetric case the onset of riddling is characterized by an unstable–unstable pair bifurcation, which also leads to unstable dimension variability in the invariant chaotic set. The nonsymmetric case exhibits a chaotic attractor, but a riddled basin occurs only at the bifurcation point, since after that the attractor becomes a chaotic saddle. We analyze the presence of unstable dimension variability in the symmetric case by computing the finite-time transverse Lyapunov exponents. We point out some consequences of those facts to the synchronization properties of coupled chaotic systems.

1. Introduction

Scientists are delighted in finding symmetries in Nature, and the mathematical models they build reflect that effort [Feynman *et al.*, 1963]. Dynamical systems have often symmetries which are translated by the existence of invariant subspaces in the corresponding state space. It is also often the case that a chaotic attractor could be embedded in this invariant subspace. One of the questions we are interested to investigate here is related to the stability of this attractor with respect to small perturbations in the transverse direction(s) to this subspace [Lai & Grebogi, 1999; Lai *et al.*, 1999b].

A remarkable dynamical phenomenon occurs if, besides the existence of this chaotic attractor, there

are other attractors off this invariant subspace; and if the transverse Lyapunov exponent of a typical orbit lying on the invariant subspace is negative. In this case, it was argued [Alexander *et al.*, 1992] that it may happen that if we pick some initial condition off the invariant subspace which generates a trajectory that asymptotes to the chaotic attractor in the invariant subspace, there are other nearby initial conditions, arbitrarily close to it, that generate trajectories which go to another attractor. We may say that the basin of the chaotic attractor is riddled with holes belonging to the basin of the other attractor. A chaotic attractor is said to have a riddled basin of attraction if the basin itself has a positive Lebesgue measure and if, for every neighborhood of every point in the basin of the attractor, there

exists a set of points with positive Lebesgue measure that asymptote to another attractor.

An immediate consequence of the existence of riddled basins of attraction is the emergence of a nearly hopeless barrier to predictability, since if we pick an initial condition belonging to the basin of the chaotic attractor, there are points arbitrarily close to it that belong to the basin of another attractor. The uncertainty exponent, which is related to the fraction of uncertain initial conditions in the state space with the size of the uncertainty, is zero in this case [Grebogi *et al.*, 1985a], so that other ways to characterize fractal riddled sets are necessary [Lai & Grebogi, 1996].

The emergence of riddled basins can be associated with a bifurcation phenomenon, more specifically an unstable–unstable pair bifurcation [Grebogi *et al.*, 1983]. A two-dimensional example of this riddling bifurcation is the collision between two repellers and a saddle — the latter being embedded in the chaotic attractor in the invariant subspace — as a system parameter passes through a critical value. After this collision, the basin of the chaotic attractor is riddled with holes belonging to an attractor off the invariant subspace [Lai *et al.*, 1996].

This paper aims to explore the connection between the existence of riddled basins of attraction and the symmetry properties of nonlinear dynamical systems. We have chosen as a model a two-dimensional map that has a symmetry-breaking parameter, in order to evidence the kind of bifurcations leading to riddling. We study the symmetric and nonsymmetric cases, analyzing their bifurcation properties as a control parameter is varied. In the symmetric case an attractor lies in an invariant subspace, and the onset of riddling is characterized by a saddle–repeller bifurcation [Lai *et al.*, 1996], in which a saddle fixed point is embedded in the chaotic attractor and two outsider repellers collide. This bifurcation is followed by the creation of an open dense set of ultra-narrow tongues anchored at the chaotic attractor on a countable infinite number of points. The complement of this set is the riddled basin of the chaotic attractor, and has positive Lebesgue measure, being a fat fractal basin [Lai, 2000]. Another feature that is present after the bifurcation is the occurrence of unstable dimension variability in the chaotic set, since there are two intertwined sets of unstable points with a different number of unstable directions [Lai & Grebogi, 2000].

This has deep implications in the shadowability properties of chaotic trajectories in the invariant set as well as in the concepts behind the modeling of physical phenomena by such dynamical systems [Lai *et al.*, 1999a], being particularly important in lattices of coupled oscillators and discrete maps [Lai *et al.*, 1999b; Barreto & So, 2000]. In this paper, the existence of unstable dimension variability after the saddle–repeller bifurcation is further verified by numerical computation of the finite-time Lyapunov exponents in the direction transversal to the invariant subspace in which lies the chaotic attractor [Kostelich *et al.*, 1997]. These exponents fluctuate about zero due to the different number of unstable directions found by a typical trajectory in the chaotic invariant set.

The nonsymmetric case, however, presents different bifurcation properties. There is also a chaotic attractor with Hénon-like leaves, bearing a saddle fixed point that collides with one of the repellers and disappears after the bifurcation, turning the attractor into a chaotic saddle. The other repeller does not interfere with the saddle–repeller bifurcation. In this case, there is riddling only at the unstable–unstable pair bifurcation. After this point there are no longer riddled sets, since the invariant set becomes a chaotic saddle [Viana & Grebogi, 2000].

This paper is organized as follows: in the second section we present a linear analysis of the map here studied, emphasizing the differences between the symmetric and nonsymmetric cases. Section 3 is devoted to a numerical analysis of the transverse finite-time Lyapunov exponent distribution for the symmetric case. The following section deals with the connection between our two-dimensional map and the synchronization properties of two nonlinearly coupled chaotic systems. Our conclusions are left to the final section.

2. Symmetry Breaking and Riddling

Chaotic dynamical systems with an invariant subspace are very useful mathematical models for physical systems with symmetries, as well as for lattices of coupled chaotic oscillators occurring in physical, biological and technological applications [Heagy *et al.*, 1994]. For networks of coupled chaotic systems the invariant subspace of interest is the synchronization manifold [Pecora *et al.*, 1997; Lai & Grebogi, 2000]. We will first discuss the case in

which there is a state space symmetry in the direction transverse to the invariant subspace.

We will analyze a class of $(N + M)$ -dimensional maps in the general form [Lai *et al.*, 1996]

$$\mathbf{x}_{n+1} = \mathbf{f}(\mathbf{x}_n), \quad (1)$$

$$\mathbf{y}_{n+1} = \varepsilon + pg(\mathbf{x}_n)\mathbf{y}_n + \text{higher order odd terms in } \mathbf{y}_n, \quad (2)$$

where $\mathbf{x} \in R^N$, $N \geq 1$ and $\mathbf{y} \in R^M$, $M \geq 1$. The invariant subspace \mathcal{M} here is given by $\mathbf{y}_n = 0$: if \mathbf{y}_0 lies in \mathcal{M} , every further iteration of the map will remain in \mathcal{M} . In this case, we assume that the N -dimensional map $\mathbf{f}(\mathbf{x})$ has a chaotic attractor in \mathcal{M} . $p > 0$ is the control parameter for this system, such that $pg(\mathbf{x}_n) \geq 0$ for all \mathbf{x} . Moreover, we require that $g(\mathbf{x}_n) = 1$, when \mathbf{x} is equal to some unstable periodic orbit of the map $\mathbf{f}(\mathbf{x})$. A low-dimensional ($N = M = 1$) realization of the above system, with a cubic nonlinearity, is

$$x_{n+1} = ax_n(1 - x_n), \quad (3)$$

$$y_{n+1} = \varepsilon + pe^{-b(x_n - \chi)^2}y_n + y_n^3, \quad (4)$$

where a and b are non-negative parameters. We will begin by considering $\varepsilon = 0$. The linear term in y is nonlinearly driven by a logistic map in x -direction. We choose χ as the fixed point of the logistic map: $\chi = 1 - (1/a)$. The set of parameter values for which the logistic map exhibits chaotic motion is a positive Lebesgue measure fractal set [Jacobson, 1981; Grebogi *et al.*, 1985c]. In particular, the choice $a = 3.8$ gives $\chi \approx 0.7368$ as an unstable fixed point embedded in an apparently chaotic attractor at $y = 0$. The $y = 0$ line is an invariant subspace of the system, as a consequence of the reflection symmetry $y \rightarrow -y$ present in Eq. (4).

The fixed points of this map (3-4) are $\mathbf{0} = (\chi, 0)$ and $\mathbf{r}_{\pm} = (\chi, y_{\pm} = \pm\sqrt{1-p})$. Linear stability analysis shows that $\mathbf{0}$ is a saddle and \mathbf{r}_{\pm} are sources (repellers) for $a > 3$ and $p < 1$ [Lai *et al.*, 1996]. It is instructive to set up $x = \chi$ and consider only the y -part of the map $y \mapsto f_0(y) = py + y^3$. For $p < 1$ these fixed points are the intersections between the map function and the 45° -line [Fig. 1(a)]. As p is increased towards 1, the repellers at y_{\pm} approach each other and eventually coalesce at $y = 0$ [Fig. 1(b)]. For $p > 1$ the repellers no longer exist and the saddle at $y = 0$ has become a repeller [Fig. 1(c)]. This is a saddle-repeller bifurcation at $p = p_c = 1$ [Fig. 2(a)], which is an

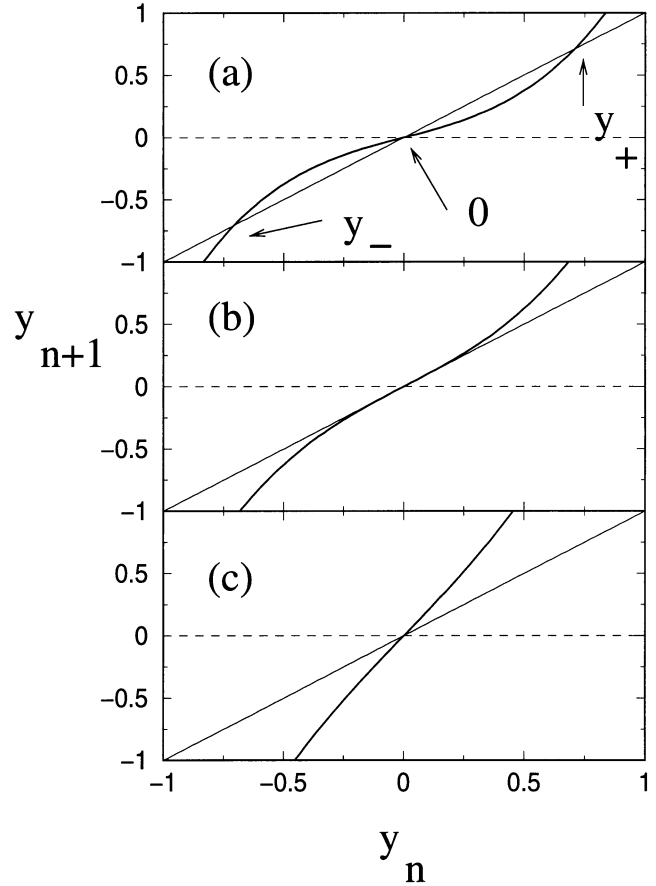


Fig. 1. Transverse map [Eq. (4)] at $x = \chi$ for $\varepsilon = 0$ and (a) $p = 0.5$, (b) $p = p_c = 1.0$ and (c) $p = 2.0$.

unstable-unstable pair bifurcation with eigenvalue $+1$ [Fig. 2(b)].

Besides these fixed points, there is another fixed point at infinity, to which asymptote orbits lie in the corresponding basin of attraction. For $p \lesssim 1$, there is a fractal basin boundary (with box-counting dimension $D_B = 1.77 \pm 0.10$, for $p = 0.99$) separating the basin of the chaotic attractor in the invariant subspace at $y = 0$ from the basin of the attractor at infinity [Fig. 3(a)]. The fractal nature of this basin boundary leads to final-state sensitivity, as evidenced by the scaling $f \sim \varpi^\alpha$ of the uncertain fraction of the state space as a function of the uncertainty ϖ in the initial conditions, where $\alpha = D - D_B$ is the uncertainty exponent. Since the dimension of the state space is $D = 2$, we have $\alpha \approx 0.22$ for that value of p . In this case, in order to reduce the uncertain fraction of initial conditions to half of its value, for example, the corresponding increase in accuracy (or decrease in ϖ) should be $\approx 96\%$. This is a characteristic behavior of fractal basin boundaries [Grebogi *et al.*, 1985a].

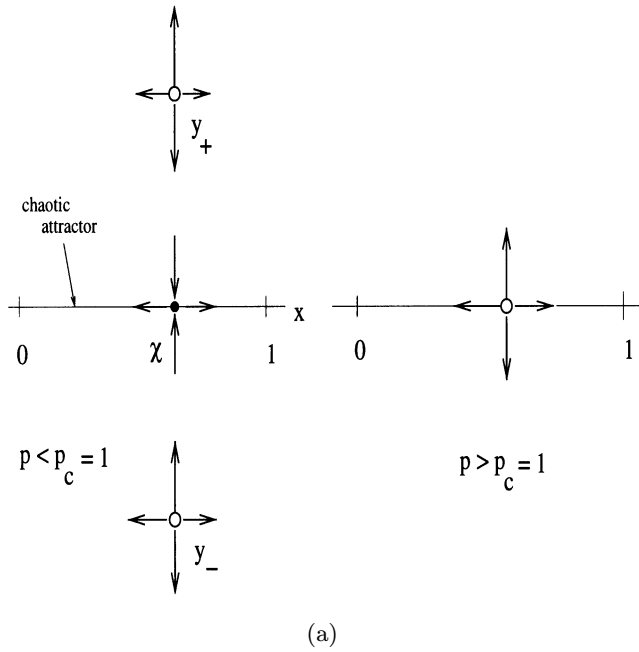


Fig. 2. (a) Saddle-repeller bifurcation (at $p_c = 1$) for the $\varepsilon = 0$ case; (b) bifurcation diagram for the corresponding y -map. Solid (dashed) lines indicate stable (unstable) fixed points.

Another remark about the dynamics in the $p \leq 1$ case is that, whereas the fixed point $\mathbf{0}$ lies in the chaotic attractor in the invariant subspace, the other points \mathbf{r}_{\pm} lie in the corresponding basin boundary [Fig. 3(a)]. So, when they coalesce at $p = p_c = 1$, this may be thought as a collision

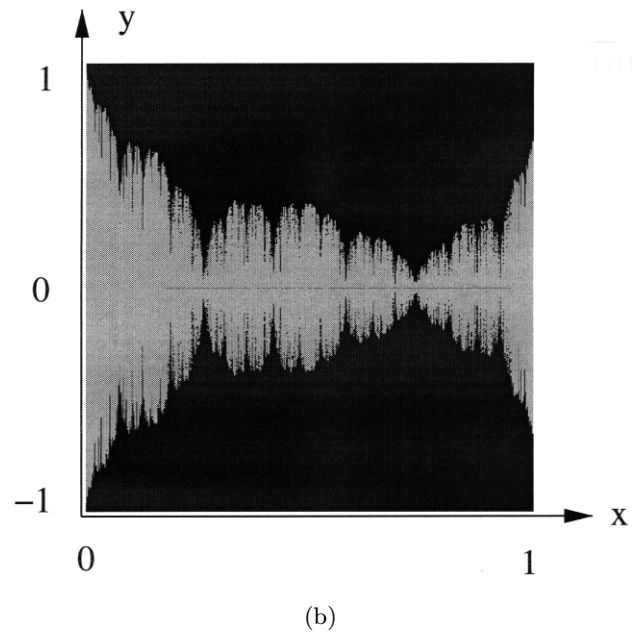
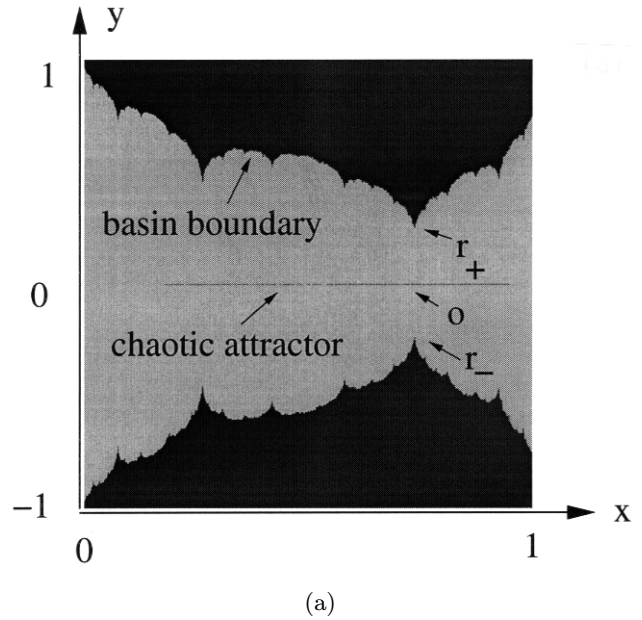


Fig. 3. Phase portraits of the map (3–4) for $a = 3.8$, $b = 5.0$, $\varepsilon = 0$, and (a) $p = 0.99$, (b) $p = 1.30$. The gray region is the basin of the chaotic attractor at $y = 0$, whereas the dark region is the basin of the attractor at infinity. In (a), the locations of the saddle and repellers are indicated by arrows.

between the chaotic attractor and its basin boundary, i.e. a boundary crisis [Grebogi *et al.*, 1983, 1985b]. On the other hand, when these points collide, every preimage of them (and there is an infinite number of such points in the invariant subspace \mathcal{M}) also suffers a collision. This causes the appearance of a tongue-like structure anchored in the chaotic

attractor in \mathcal{M} . An open set ($|y| > 1$) that intersects the transverse unstable manifold of χ , will approach χ asymptotically for the inverse process. These inverse images intersect the tongue that appeared at $x = \chi$ for $p = p_c = 1$, if the initial open set is large enough. There is a denumerable infinite number of these tongues anchored at $y = 0$, i.e. the points on which the tongues are anchored form a dense open set in the invariant subspace \mathcal{M} . The complement of this set has positive Lebesgue measure, comprising a nondenumerable infinite number of saddles [Lai *et al.*, 1996].

The emergence of a tongue structure is illustrated in Fig. 3(b), for $p \gtrsim p_c = 1$. The tongues' widths decrease geometrically, but at least their thicker parts are visible. Due to the formation of tongues anchored at repellers, the basin of the chaotic attractor, lying in its complement, is a positive Lebesgue measure set. This characterizes the riddling of the basin of the attractor in \mathcal{M} . For every initial condition that asymptotes to it, there are other initial conditions, arbitrarily close to it, that asymptote to the attractor at infinity. In this case, decreasing the uncertainty ϖ in the determination of the initial condition does not lead to any reduction of the uncertain fraction of the state space, the exponent α being equal to zero. Moreover, there is a sequence of densely intertwined saddles and repellers in the chaotic attractor at $y = 0$. Since the dimension of the unstable manifold is different for saddles and repellers, it results in unstable dimension variability for the chaotic invariant set. Therefore, for this case at least, the onset of riddling at $p = p_c = 1$ indicates also the onset of unstable dimension variability. We remark, however, that not all riddled basins characterize invariant sets with this property.

Now, what does occur if we allow ε to be different from zero? Firstly, the symmetry in y -direction is broken and the $y = 0$ line is no longer an invariant subspace, so that ε is a symmetry-breaking parameter. For small values of ε , the chaotic attractor becomes now a fractal Hénon-like structure of leaves (with box-counting dimension $D_B = 1.74 \pm 0.15$ for $p = 0.99$ and $\varepsilon = 0.01$, see Fig. 4). There is an infinite number of unstable periodic orbits embedded in this chaotic attractor. If the symmetry-breaking parameter is small enough, it is reasonable to assume that most periodic orbits that are unstable for $\varepsilon = 0$ remain so under this perturbation. However, the location of these unstable points will

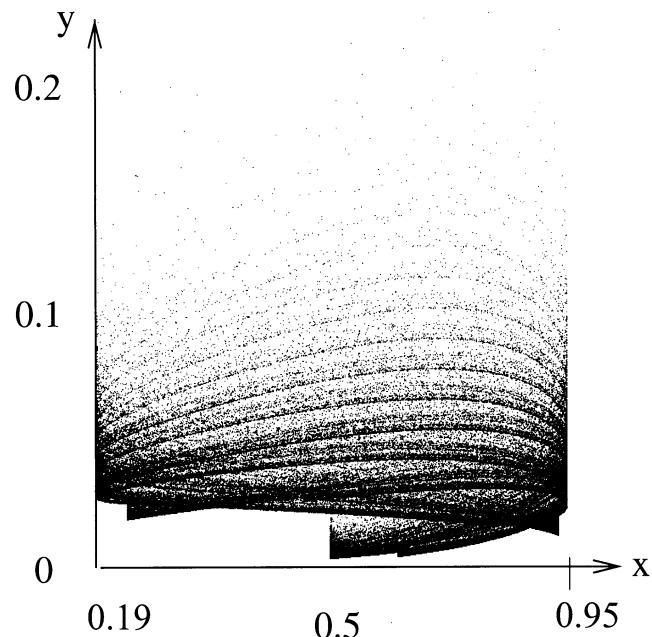


Fig. 4. Phase portrait of the map (3–4) for $a = 3.8$, $b = 5.0$, $\varepsilon = 0.01$ and $p = 0.99$.

change over a strip of width ε centered at $y = 0$ [Lai, 2000].

In order to analyze the behavior of the fixed points in this case, we consider again the y -part of the map at the unstable fixed point $x = \chi$: $y \mapsto f_\varepsilon(y) = \varepsilon + py + y^3$. For subcritical p -values, the former saddle at the origin is displaced, by a quantity proportional to ε , to the point $y = y_0$; whereas the repellers are likewise displaced to new values of y_+ and y_- [Fig. 5(a)]. As p increases, due to this ε -offset, the saddle begins to approach the repeller and they eventually coalesce when

$$p = \tilde{p}_c = 1 - 3 \left(\frac{\varepsilon}{2} \right)^{2/3} < p_c = 1 \quad (5)$$

at the point $y_c = (\varepsilon/2)^{1/3}$, such that $y_0 < y_c < y_+$ [Fig. 5(b)]; and the other repeller is located at $y_- = -2y_c$. For $p \gtrsim \tilde{p}_c$ only the latter fixed point remains, whereas the saddle-repeller pair disappears leaving a narrow channel between $f_\varepsilon(y)$ and the 45° -line, through which orbits spend considerable time until they are ejected toward larger y -values [Fig. 5(c)]. Moreover, y_- approaches monotonically the origin as p increases further.

This is an unstable–unstable pair bifurcation different from the one just described for vanishing ε [Fig. 6(a)], and it is similar to that studied in the other two-dimensional map, where unstable dimension variability has been previously described

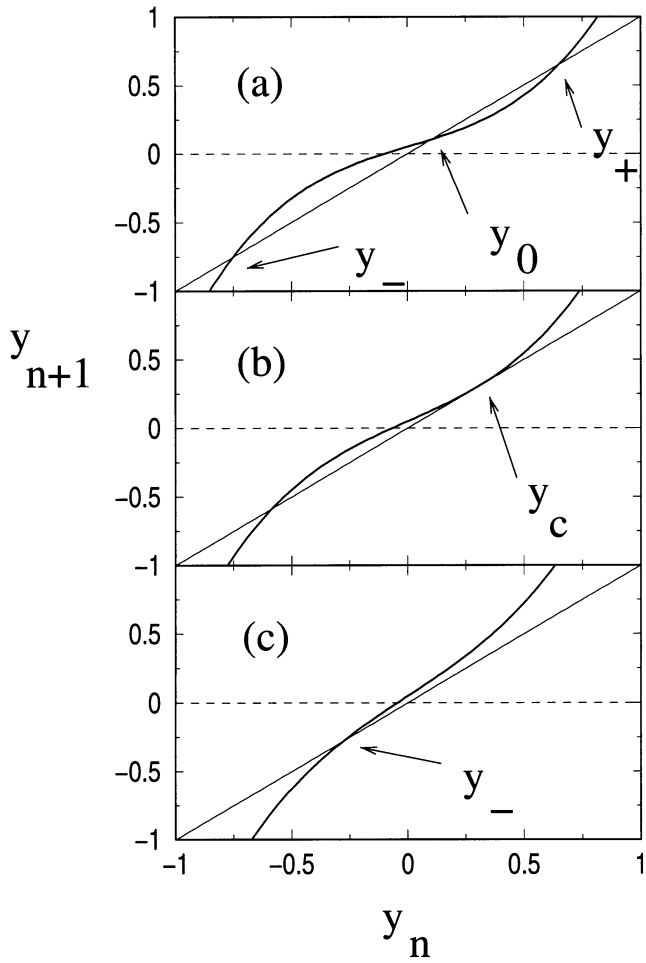


Fig. 5. Transverse map at $x = \chi$ for $\varepsilon = 0.05$ and (a) $p = 0.5$, (b) $p = \tilde{p}_c \approx 0.7434$ and (c) $p = 1.1$.

[Grebogi *et al.*, 1983, 1985b; Viana & Grebogi, 2000]. In fact, if only the y -map is taken into account, it is a backward tangent bifurcation at $y = y_c$ [Fig. 6(b)]. Let us focus our attention on this new bifurcation: exactly at the point $p = \tilde{p}_c$, where the saddle and repeller coalesce, a tongue-like structure is again expected to appear. This is the onset of both riddling and unstable dimension variability. However, for $p > \tilde{p}_c$ the saddle-repeller pair has disappeared, and only the repeller at y_- survives. As in the symmetric case, in the subcritical case the repellers y_+ and y_- belong to the boundaries of the basin of the chaotic attractor containing the saddle y_0 . So, the tangent bifurcation at \tilde{p}_c means a collision of the chaotic attractor with its basin, which turns the attractor into a chaotic saddle located at the $y > 0$ half-plane. A typical orbit in this nonattracting saddle is a chaotic transient.

Hence, a riddled basin occurs only for $p = \tilde{p}_c$, when ε is not zero. This is a riddling bifurcation,

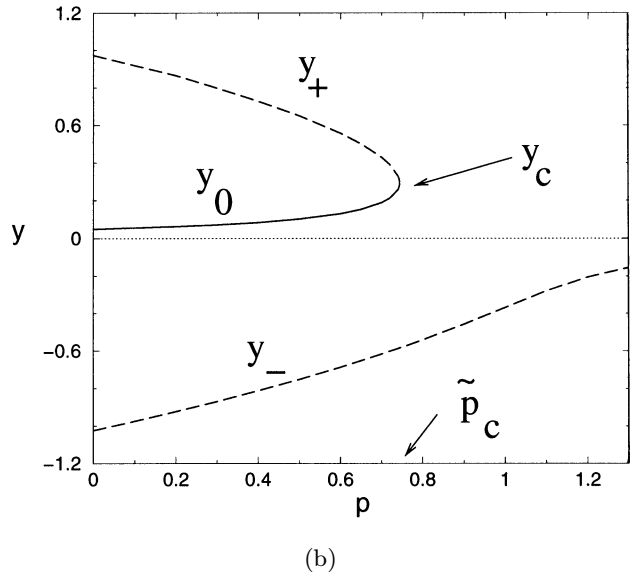
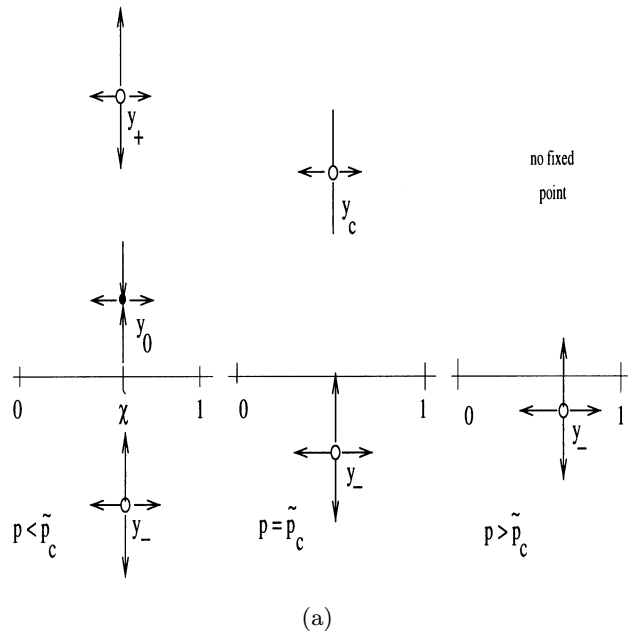


Fig. 6. (a) Saddle-repeller bifurcation (at $p = \tilde{p}_c$) for the $\varepsilon \neq 0$ case; (b) bifurcation diagram for the corresponding y -map. Solid (dashed) lines indicate stable (unstable) fixed points.

but in this case riddling is no longer a “typical” effect, since it occurs for a set of system parameters that has zero Lebesgue measure. The tongues originating immediately after the unstable–unstable pair bifurcation continue to exist, and have finite width [Grebogi *et al.*, 1985b]. Trajectories arising from initial conditions belonging to the former basin of the chaotic attractor will approach its remnant and wander in its vicinity, until they enter in a tongue and escape toward the attractor at infinity.

Since the openings of the tongues are very small for $p \gtrsim \tilde{p}_c$, it takes an exponentially growing time for an orbit to enter in such tongues. The duration of these super persistent transients has been studied by several authors [Grebogi *et al.*, 1983, 1985b; Lai *et al.*, 1996].

3. Finite Time Lyapunov Exponents

In both symmetric and nonsymmetric cases, the emergence of unstable dimension variability is due to the appearance of an alternating sequence of saddles and repellers along the chaotic invariant set, and whose onset is the unstable–unstable pair bifurcation of one of those types described in the previous section. This invariant set is a chaotic attractor, in the symmetric case, and a chaotic saddle, in the nonsymmetric one. A typical trajectory in either chaotic set evolves along one expanding (unstable) dimension for some time, and along two unstable dimensions for other times, and so on. Therefore, the dynamics in the transversal direction, corresponding to the second exponent, will alternatively shrink and expand for finite amounts of time [Lai & Grebogi, 2000]. The contraction or expansion rates along a trajectory segment are quantified by the finite-time Lyapunov exponents.

The k th time- n Lyapunov exponent is defined as [Kostelich *et al.*, 1997]

$$\lambda_k(x_0, y_0; n) = \frac{1}{n} \ln \|\mathbf{DF}^n(x_0, y_0) \cdot \mathbf{v}_k\|, \quad (6)$$

where $\mathbf{DF}^n(\mathbf{x})$ is the Jacobian matrix of the n -times iterated map, and \mathbf{v}_k is one of its singular values. In the limit $n \rightarrow \infty$ we obtain the usual Lyapunov exponents.

In this section we will consider only the case $\varepsilon = 0$. The case in which the symmetry-breaking parameter is not vanishing has been considered in a previous paper, for a similar map [Viana & Grebogi, 2000]. From the Jacobian matrix of the map (3–4), it follows that the time- n Lyapunov exponents are

$$\lambda_1(x_0, y_0; n) = \frac{1}{n} \sum_{i=1}^n \ln[a(1 - 2x_i)], \quad (7)$$

$$\lambda_2(x_0, y_0; n) = \frac{1}{n} \sum_{i=1}^n \ln[pe^{-b(x_i - \chi)^2} - 3y_i^2], \quad (8)$$

corresponding to eigenvectors pointing to the x - and y -directions, respectively. The infinite-time limit of

$\lambda_1(n)$, for $a = 4$, is known to be $\ln 2$ [Gulick, 1990]. The same limit, when applied to the y -direction, gives the transversal Lyapunov exponent

$$\lim_{n \rightarrow \infty} \lambda_2(x_0, y_0; n) = \lambda_T, \quad (9)$$

which determines the transversal stability of orbits lying in the invariant subspace at $y = 0$ [Lai *et al.*, 1999b].

The presence of unstable dimension variability for $p \geq p_c = 1$ causes the transversal time- n exponent $\lambda_2(n)$ to fluctuate about zero. In order to characterize statistically this dispersion, we have obtained numerically a probability distribution for the transversal n -time exponent, written $P(\lambda_2(n), n)$ [Kostelich *et al.*, 1997]. We interpret $P(\lambda_2(n), n)d\lambda_2$ as the probability that $\lambda_2(n)$ lies between λ_2 and $\lambda_2 + d\lambda_2$ for finite n . The initial conditions (x_0, y_0) are randomly chosen according to the natural measure of the chaotic attractor. If $F(\lambda_2)$ is a given function of this exponent, its average with respect to this probability distribution is given by

$$\begin{aligned} \langle F(\lambda_2(\mathbf{x}_0, n)) \rangle &= \int_{-\infty}^{+\infty} F(\lambda_2(\mathbf{x}_0, n))P(\lambda_2(\mathbf{x}_0, n), n)d\lambda_2, \quad (10) \end{aligned}$$

provided we adopt the normalization

$$\int_{-\infty}^{+\infty} P(\lambda_2(\mathbf{x}_0, n), n)d\lambda_2 = 1. \quad (11)$$

Remember that, for $p \geq 1$, an orbit initially placed in the neighborhood of the chaotic attractor may enter a tongue, and after some (possibly very large) time, it eventually asymptotes to the attractor at infinity. We generate a long chaotic transient, from which we take a large number of nonoverlapping consecutive sections of length n . To each of these sections, starting from different orbit points, we compute the time- n exponent according to Eq. (8) and make a frequency histogram.

In Fig. 7, we depict some examples of probability distributions obtained according to the numerical procedure described above, for a chaotic attractor in the invariant manifold at $y = 0$, and for which we choose $a = 4$. In all cases, we observe that the approximate shape of the curves is Gaussian, but with unequal tails on both sides. The negative tail is more Gaussian-like, whereas the positive tail ends up quite abruptly. The width of the distribution

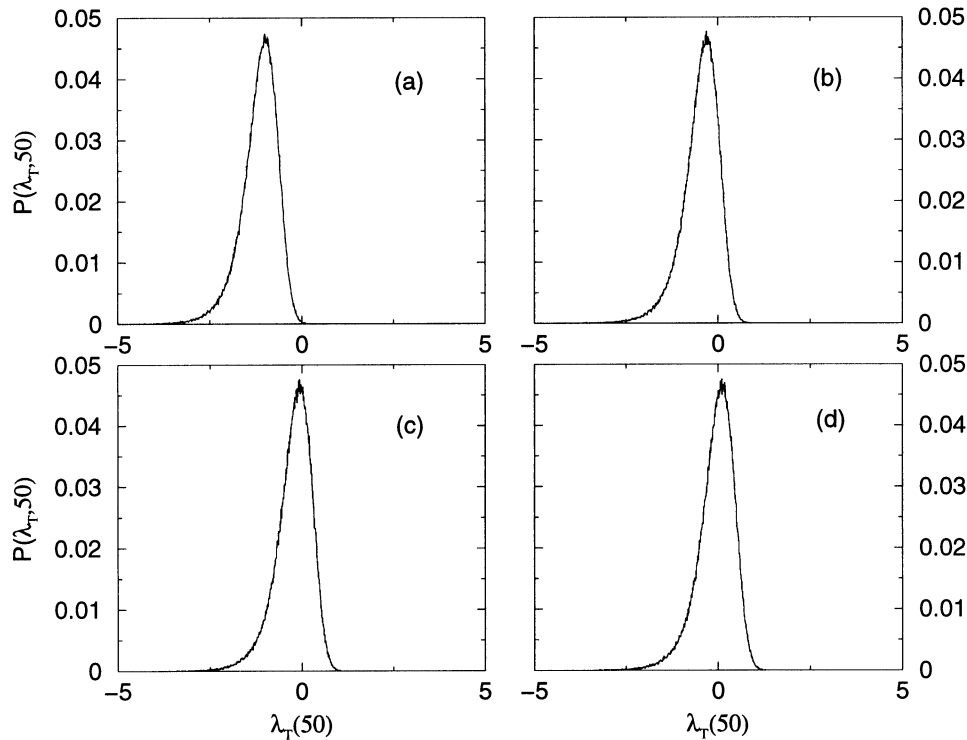


Fig. 7. Probability distribution for the transverse time-50 Lyapunov exponents for $a = 4.0$, $b = 5.0$, $\varepsilon = 0$ and (a) $p = 1.0$, (b) $p = 2.0$, (c) $p = 2.5$, (d) $p = 3.0$.

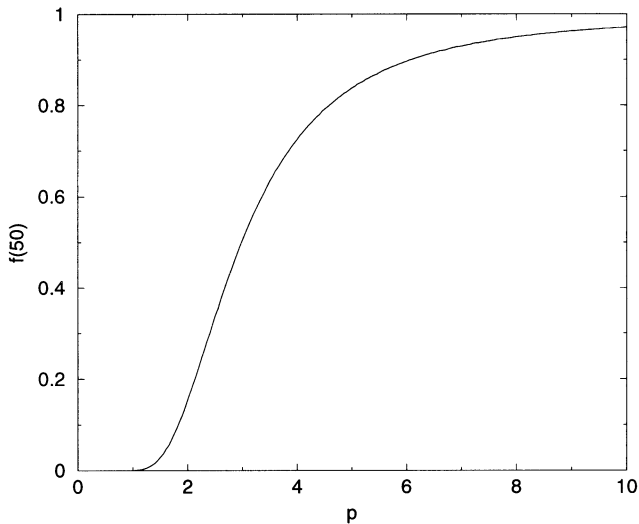


Fig. 8. Fraction of positive transverse time-50 Lyapunov exponents as a function of p , for $a = 4.0$, $b = 5.0$ and $\varepsilon = 0$.

seems to be independent of p . For $p < 1$, no finite-time transversal exponent could be positive because there are only transversally stable fixed points on the chaotic attractor. As p increases past this value, however, the number of positive transversal exponents builds up because more and more periodic

orbits on the chaotic attractor lose transversal stability. This is clearly shown in Fig. 8, where we depict the fraction of the positive time- n transverse exponents,

$$f(n) = \int_0^\infty P(\lambda_2(\mathbf{x}_0, n), n) d\lambda_2, \quad (12)$$

as a function of p . We see a monotonic increase of p from $p_c = 1$, which saturates on the limiting value $f = 1$, for large p . This means that, for values of p far enough from the bifurcation point, almost all points on the attractor become repellers. The shape of the curve in Fig. 8 suggests a kind of integrated probability distribution, that was found to be related to the cumulative frequency histogram for $P(\lambda_2)$ [Viana & Grebogi, 2000].

4. Coupled Synchronized Maps

The map introduced in Sec. 2 may be regarded in another context. It may describe the synchronization properties of coupled maps having chaotic trajectories, since in this case it is possible to define a synchronization manifold [Heagy *et al.*, 1994; Pecora *et al.*, 1997]. One of the coordinates would

describe the situation in the synchronization manifold, whereas the other coordinate describes the behavior along its transversal direction. Loss of transversal stability of the synchronized state is thus related to the properties of the corresponding part of the map.

Let us consider two identical and nonlinearly coupled linear maps

$$u_{n+1} = \frac{a}{2} u_n + \mathcal{U}(u_n, w_n), \tag{13}$$

$$w_{n+1} = \frac{a}{2} w_n + \mathcal{W}(u_n, w_n), \tag{14}$$

where \mathcal{U} and \mathcal{W} are given by

$$\begin{aligned} \mathcal{U}(u_n, w_n) = & \frac{a}{2} \left[w_n - \frac{1}{\sqrt{2}} (u_n + w_n)^2 \right] \\ & + \mathcal{C}(u_n, w_n), \end{aligned} \tag{15}$$

$$\begin{aligned} \mathcal{W}(u_n, w_n) = & \frac{a}{2} \left[u_n - \frac{1}{\sqrt{2}} (u_n + w_n)^2 \right] \\ & - \mathcal{C}(u_n, w_n), \end{aligned} \tag{16}$$

where

$$\begin{aligned} \mathcal{C}(u_n, w_n) = & \frac{\varepsilon}{\sqrt{2}} + \frac{1}{4} (u_n - w_n)^2 + \frac{p}{2} (u_n - w_n) \\ & \times \exp \left[-b \left(\frac{1}{\sqrt{2}} (u_n + w_n) - \chi \right)^2 \right], \end{aligned} \tag{17}$$

with $a > 0$, $b > 0$, $p > 0$, $\varepsilon \geq 0$ and $\chi > 0$ as constant parameters.

The synchronization manifold \mathcal{M} in the phase plane is the straight line $u = w$, the corresponding transverse subspace being likewise one-dimensional. The transversal stability of orbits lying in \mathcal{M} is investigated by tracking the evolution of a small segment transverse to \mathcal{M} under the dynamics of the model. If the orbit is transversely stable (unstable) this segment will shrink (grow) with time, the corresponding rate of contraction (expansion) being the (infinite time) transverse Lyapunov exponent λ_T given by Eq. (9). If $\lambda_T > 0$ typical orbits in \mathcal{M} are transversally unstable [Lai *et al.*, 1999b]. In order to study the dynamics of the coupled system in the synchronization manifold \mathcal{M} and its transverse subspace, we introduce orthogonal coordinates corresponding to a 45° clockwise rotation of coordinates

$$x = \frac{1}{\sqrt{2}} (u + w), \quad y = \frac{1}{\sqrt{2}} (u - w), \tag{18}$$

so that y turns to be the dynamical variable along the transverse direction and \mathcal{M} is now given by $y = 0$. The coupled system in these rotated coordinates is the map (3)–(4).

5. Conclusions

Riddling of basins of attraction is a phenomenon occurring for a large class of dynamical systems, since the conditions for its existence are often met. One of these conditions is the existence of an invariant manifold. We have considered in this paper a two-dimensional map where the existence of a spatial symmetry implies the existence of a synchronization manifold for two nonlinearly coupled chaotic maps. We have studied the behavior of this dynamical system when a spatial symmetry is present ($\varepsilon = 0$) or broken ($\varepsilon \neq 0$). In the latter case, it is still possible to relate the chaotic attractor, that is no longer restricted to an invariant subspace, to a generalized synchronization state in which there appears an emergent set [Barreto & So, 2000].

For the nonsymmetric case we have considered an unstable–unstable pair bifurcation when a system parameter is varied. We have found that, precisely at the bifurcation point, riddled basins also exist for this system, even though it does not have an invariant subspace. This is riddling, but only at the riddling bifurcation parameter value, in contrast with the symmetric case ($\varepsilon = 0$). In both situations, there is unstable dimension variability at the riddling bifurcation.

In summary, we have described in this paper two mathematical situations in which riddling accompanies unstable dimension variability. While in the symmetric case this was found to be a robust phenomenon, numerically confirmed by explicit computation of finite-time Lyapunov exponents, in the nonsymmetric case this is an exceptional situation and unlikely to be found in many physical systems.

Acknowledgments

We acknowledge helpful discussions with S. E. S. Pinto, E. Macau, P. So and E. Barreto. This work was made possible by partial financial support from National Science Foundation (Division of International Programs) and CNPq (Conselho Nacional de

Desenvolvimento Científico e Tecnológico) – Brazil, through a joint research collaboration project. It was also supported in part by ONR (Physics).

References

- Alexander, J. C., Yorke, J. A., You, Z. & Kan, I. [1992] “Riddled basins,” *Int. J. Bifurcation and Chaos* **2**, 795–813.
- Barreto, E. & So, P. [2000] “Mechanisms for the development of unstable dimension variability and the breakdown of shadowing in coupled chaotic systems,” *Phys. Rev. Lett.* **85**, 2490–2493.
- Feynman, R. P., Leighton, R. B. & Sands, M. [1963] *The Feynman Lectures on Physics* (Addison Wesley, NY), Vol. 1, Section 11-1.
- Grebogi, C., Ott, E. & Yorke, J. A. [1983] “Fractal basin boundaries, long-lived chaotic transients, and unstable-unstable pair bifurcation,” *Phys. Rev. Lett.* **50**, 935–938.
- Grebogi, C., Ott, E. & Yorke, J. A. [1985a] “Fractal basin boundaries,” *Physica* **D17**, 125–153.
- Grebogi, C., Ott, E. & Yorke, J. A. [1985b] “Super persistent chaotic transients,” *Ergod. Th. Dyn. Syst.* **5**, 341–372.
- Grebogi, C., McDonald, S. W., Ott, E. & Yorke, J. A. [1985c] “The exterior dimension of fat fractals,” *Phys. Lett.* **A110**, 1–4.
- Gulick, D. [1990] *Directions in Chaos* (McGraw Hill, NY).
- Heagy, J. F., Carroll, T. L. & Pecora, L. M. [1994] “Synchronous chaos in coupled oscillator systems,” *Phys. Rev.* **E50**, 1874–1885.
- Jacobson, M. V. [1981] “Absolutely continuous invariant measures for one-parameter families of one-dimensional maps,” *Commun. Math. Phys.* **81**, 39–88.
- Kostelich, E. J., Kan I., Grebogi, C., Ott, E. & Yorke, J. A. [1997] “Unstable dimension variability: A source of nonhyperbolicity in chaotic systems,” *Physica* **D109**, 81–90.
- Lai, Y.-C. & Grebogi, C. [1996] “Characterizing riddled fractal sets,” *Phys. Rev.* **E53**, 1371–1374.
- Lai, Y.-C., Grebogi, C., Yorke, J. A. & Venkataramani, S. C. [1996] “Riddling bifurcation in chaotic dynamical systems,” *Phys. Rev. Lett.* **77**, 55–58.
- Lai, Y.-C. & Grebogi, C. [1999] “Modeling of deterministic chaotic systems,” *Phys. Rev.* **E59**, 2907–2910.
- Lai, Y.-C., Grebogi, C. & Kurths, J. [1999a] “Modeling of coupled chaotic oscillators,” *Phys. Rev. Lett.* **82**, 4803–4806.
- Lai, Y.-C., Lerner, D., Williams, K. & Grebogi, C. [1999b] “Unstable dimension variability in coupled chaotic systems,” *Phys. Rev.* **E60**, 5445–5454.
- Lai, Y.-C. [2000] “Catastrophe of riddling,” *Phys. Rev.* **E62**, R4505–R4508.
- Lai, Y.-C. & Grebogi, C. [2000] “Obstruction to deterministic modeling of chaotic systems with invariant subspace,” *Int. J. Bifurcation and Chaos* **10**, 683–693.
- Pecora, L. M., Carroll, T. L., Johnson, G. A., Mar, D. J. & Heagy, J. F. [1997] “Fundamentals of synchronization in chaotic systems, concepts, and applications,” *Chaos* **7**, 520–543.
- Viana, R. L. & Grebogi, C. [2000] “Unstable dimension variability and synchronization of chaotic systems,” *Phys. Rev.* **E62**, 462–468.